



3 8006 10058 4039

CoA Memo No. 101

THE COLLEGE OF AERONAUTICS
CRANFIELD

Shock Reflection and Surface Effects in
the Shock Tube

by

J. R. Busing and John F. Clarke



S u m m a r y

A thin-film resistance thermometer, mounted on the end-wall of a shock tube, is used to record surface temperatures and heat transfer rates following reflection of the primary shock wave.

This information is combined with the results of theoretical investigations to produce simultaneous information about surface accommodation effects and gas thermal conductivities at high pressures and moderate temperatures.

This is a preprint of a paper to be presented at the 7th AGARD Colloquium on "Recent Advances in Aerothermochemistry", Oslo, Norway, May 1966.

1. Introduction

When the primary shock wave in a simple shock tube reflects from the closed end of that tube a region of hot, high pressure, stagnant gas is left behind in contact with the, initially, cold solid surface. What is virtually a one-dimensional unsteady heat conduction situation between the hot gas and the cold solid is therefore created and, as such, has been exploited by a number of workers. Amongst these we may mention Hansen (1959, 1960), Lauver (1964), Peng & Ahtye (1961) and Friedman & Fay (1965) all of whom have been interested in measurement of the thermal conductivity of the hot gas. More recently Baganoff (1965) has measured pressures on the end wall in a similar situation.

The measurements of thermal conductivity have all been made by means of a thin-film platinum resistance thermometer, mounted in the centre of the shock tube end-wall. The gauge output, which is proportional to the temperature of the solid, is displayed on an oscilloscope and generally has the form indicated in fig 1. when a reasonably slow (greater than about 10 $\mu\text{sec/cm}$) sweep speed is used. At B the simple heat conduction situation has broken down due to the various wave interactions occurring in the tube, but between A and B there is generally a fairly constant oscilloscope output which can be related to a surface temperature rise ΔT_{sa} . This temperature rise can be used to determine the thermal conductivity of the gas.

Between points O and A the oscilloscope trace rises smoothly to its asymptotic level. The time interval over which this occurs is far too long to be accounted for by the rise-time of the electronic recording apparatus and it has already been pointed out (Clarke, 1962) that the behaviour of the portion OA of the trace is intimately connected with the effectiveness of energy transfer to the solid surface. The paper just referred to established the form of OA theoretically in a small-disturbance situation, for which the initial hot-gas / cold-solid temperature difference was small. Experimental situations almost always violate this condition. However, we show that the form of OA is, to good accuracy, unaffected by this fact. Certain unique aspects of the particular energy transfer process involved in OA are discussed and then

exploited in the experiments. Experimental results give thermal conductivities for air and accommodation coefficients for an air / platinum combination, the latter at much higher pressures than those normally found in experimental evaluations. Gas temperature levels generally are below those for which the effects of excitation of internal molecular vibrations, or of changes in chemistry, are significant.

2. Theory

It is apparent from the work of Goldsworthy (1959) or Clarke (1960) that, to first order accuracy, the pressure in the thermal boundary layer near the wall may be taken to be constant in both space and time. Baganoff's (1965) experiments show that p measured at the wall does vary a little with time in circumstances such as those under consideration here (broadly, circumstances in which the gas behaves "ideally") and confirm the view that pressure variations have only a second-order influence on the thermal layer. The viscous dissipation in the layer is also negligible so that, with the additional assumption of an ideal gas, the energy equation becomes

$$\rho C_p \frac{DT}{Dt} = \frac{\partial}{\partial x} \left(k \frac{\partial T}{\partial x} \right) . \quad 1$$

p , ρ and T are the gas pressure, density and temperature, respectively, whilst k and C_p are the thermal conductivity and (constant) specific heat at constant pressure. D/Dt is the usual convective operator.

We assume that the gas occupies the half space to the right of $x = 0$. The solid is assumed to occupy the complete half-space $x < 0$. Its temperature, T_s , satisfies the equation

$$\frac{\partial T_s}{\partial t} = \kappa_s \frac{\partial^2 T_s}{\partial x^2} \quad 2$$

where κ_s , the diffusivity, is assumed constant. Since the temperature-rises encountered in the solid never exceed about 50°C this is a most reasonable assumption.

The energy flux must be continuous at the interface, so that

$$\left(k \frac{\partial T}{\partial x} \right)_{x=0} = \left(k_s \frac{\partial T_s}{\partial x} \right)_{x=0} , \quad 3$$

where k_s is the (constant) thermal conductivity of the solid. In addition the gas temperature-jump condition requires that

$$\left(\Gamma \frac{\partial T}{\partial x} \right)_{x=0} = (T - T_s)_{x=0} , \quad 4$$

where Γ is related to the accommodation coefficient r as follows;

$$\Gamma = \frac{2-r}{r} .1. \quad 5$$

Here l is the appropriate free path for the transfer of energy through the gas. We can write

$$l = 2k/\rho\Omega C_v, \quad 6$$

(see e.g. Clarke & McChesney, 1964) where C_v is the (constant) specific heat at constant volume and Ω is the arithmetic mean molecular speed. We remark that Ω is proportional to $T^{\frac{1}{2}}$.

For times greater than about 100 molecular collision time intervals after shock reflection from the end wall (i.e. for times greater than about 10^{-2} μ sec) the shock wave is sufficiently far away from the thermal layer for the latter to be considered as if it existed in a semi-infinite expanse of gas. Accordingly we can put

$$T \rightarrow T_\infty \quad \text{as} \quad x \rightarrow \infty, \quad t > 0, \quad 7$$

where T_∞ is the gas temperature behind the reflected shock. For the solid

$$T_s \rightarrow T_0 \quad \text{as} \quad x \rightarrow -\infty, \quad t > 0, \quad 8$$

where T_0 is the initial (room) temperature of the solid.

It is convenient to transform from Eulerian x, t coordinates into Lagrangian ψ, t coordinates in eq.1, where

$$\psi = \int_0^x \rho(\bar{x}, t) d\bar{x}. \quad 9$$

Eq.1 becomes

$$\frac{\partial T}{\partial t} = \frac{\partial}{\partial \psi} \left(\frac{\rho k}{C_p} \frac{\partial T}{\partial \psi} \right) \quad 10$$

and conditions 3, 4 and 7 transform into

$$\left(\rho k \frac{\partial T}{\partial \psi} \right)_{\psi=0} = \left(k_s \frac{\partial T_s}{\partial y} \right)_{x=0}, \quad 11$$

$$\left(\rho \Gamma \frac{\partial T}{\partial \psi} \right)_{\psi=0} = T_{\psi=0} - T_{s_{x=0}}, \quad 12$$

$$T \rightarrow T_\infty \quad \text{as} \quad \psi \rightarrow \infty, \quad t > 0. \quad 13$$

We shall assume that k is proportional to T ; then ρk is proportional to the pressure and is therefore constant. The constant β is defined so that

$$\rho k = \beta C_p. \quad 14$$

Eqs.5 and 6 show that

$$\rho\Gamma = \left(\frac{2-r}{r}\right) \left(\frac{2k}{\Omega C_V}\right) . \quad 15$$

The last group of terms is proportional to $T^{\frac{1}{2}}$. under the foregoing assumptions whence $\rho\Gamma$ would be likewise dependent upon T if r was constant. However, we have no information about the constancy or otherwise of r in the particular circumstances of the present experiments and we therefore propose to assume that $\rho\Gamma$ is constant. At least we should be justified in assuming a suitable constant mean value for $\rho\Gamma$, evaluated at an average temperature. It is in this spirit that the eventual evaluation of r will be carried out. To emphasise this assumption we shall write

$$\rho\Gamma = (\rho\Gamma)_{av} = \text{constant} \quad 16$$

where appropriate.

Eqs.2 and 10 together with conditions 8 and 11 - 13 are now a set of linear equations and boundary conditions. Addition of the initial value information that

$$T_S = T_0 ; \quad x < 0 , \quad t \leq 0 ; \quad 17$$

$$T = T_\infty (> T_0) ; \quad x > 0 , \quad t \leq 0 ; \quad 18$$

produces an initial- and boundary-value problem which is easily solved by Laplace transform methods. Denoting the transform of a problem by a bar ($\bar{\quad}$) over the relevant symbol we find that

$$\bar{T} = \bar{s}^{-1} T_\infty + A(\bar{s}) \exp(-\sqrt{\bar{s}/\beta} \psi) , \quad 19$$

$$\bar{T}_S = \bar{s}^{-1} T_0 + B(\bar{s}) \exp(\sqrt{\bar{s}/\kappa_S} x) , \quad 20$$

where \bar{s} is the (complex) transform variable and $A(\bar{s})$ and $B(\bar{s})$ are two functions to be determined from conditions 11 and 12. We find that

$$A(\bar{s}) = -QB(\bar{s}) \quad 21$$

$$B(\bar{s}) = \bar{s}^{-1} \Delta T \{1 + Q + (\rho\Gamma)_{av} Q \sqrt{\bar{s}/\beta}\}^{-1} \quad 22$$

where $\Delta T \equiv T_\infty - T_0$, 23

$$Q \equiv \sqrt{\frac{\rho_S k_S C_S}{\rho k C_P}} , \quad 24$$

and ρ_S, C_S are the density and specific heat of the solid.

The thin-film thermometer enables us to measure T_s at $x = 0$ and, with the addition of an analogue network, the value of $k_s \partial T_s / \partial x$ at $x = 0$ too. Using the symbol \supset to denote "has the transform" we find that

$$\Delta T_s \equiv T_{s_{x=0}} - T_o \supset B(\xi) \subset \frac{\Delta T}{1+Q} \left\{ 1 - e^{t/\tau} \text{Erfc} \sqrt{t/\tau} \right\}, \quad 25$$

$$q_s \equiv \left(k_s \frac{\partial T_s}{\partial x} \right)_{x=0} \supset k_s \sqrt{\xi/k_s} B(\xi) \subset \frac{Q \Delta T}{1+Q} \sqrt{\frac{\rho k C_p}{\tau}} e^{t/\tau} \text{Erfc} \sqrt{t/\tau}. \quad 26$$

Erfc is the complementary error function (the transforms can be found in Erdélyi et al, (1954) and (τ) is a time characteristic of the effectiveness of the surface accommodation processes. It has the value

$$\tau = \left(\frac{Q}{1+Q} \right)^2 \frac{(\rho \Gamma)_{av}^2}{\beta}. \quad 27$$

The result given in eq.25 is formally identical with the one given by Clarke (1962), which was obtained on the assumption of constant gas properties, including the density, and helps to explain the good agreement found with the limited experimental data given in that paper.

Fig.2 shows a plot of the function $1 - \exp(t/\tau) \text{Erfc} \sqrt{t/\tau}$ and exhibits the fact that the function approaches its asymptotic value extremely slowly. This is of considerable experimental importance for the following reasons. First, if the experiments are to provide a reasonable estimate of the time scale τ it is essential to have a clear picture of the ΔT_s trace when $t \approx \tau$. Second, in order to make these measurements, as well as those needed for evaluation of thermal conductivity, it is essential to know the asymptotic value of ΔT_s for $t \gg \tau$. Since it is quite essential to make all measurements from a single run in the shock tube the two requirements are not compatible with the use of a single trace, nor is it entirely satisfactory to display the same output, using fast and slow sweep speeds, on the two beams of a double-beam oscilloscope. Although the latter does help to fix the ordinate scale on the ΔT_s trace, experience has shown that the fitting of the theoretical curve to the experimental record by stretching or contracting the abscissae does not lead to good accuracy in the measurement of τ . However, by using an analogue network to measure the heat-transfer rate q_s (a brief description is given below), and displaying both ΔT_s and q_s outputs simultaneously

with the same time scale, these difficulties can be overcome in a rather satisfactory way which serves also to provide a fairly rigorous experimental test of the theory.

The method to be used relies upon the similarity of the temperature and heat-transfer-rate signals (see ΔT_s and q_s in eqs.25 and 26). It is important to observe that such similarity is unique and occurs only when accommodation effects are present. This can be seen as follows.

It is required to find two functions ΔT_s and q_s which behave similarly with respect to the time variable. Therefore in the most general circumstances we must write

$$\left. \begin{aligned} q_s &= f(t) , \\ \Delta T_s &= a + b f(t) , \end{aligned} \right\} \quad 28$$

where a and b are constants. Taking Laplace transforms this means that

$$\bar{q}_s = \left(k_s \frac{\partial \bar{T}_s}{\partial x} \right)_{x=0} = \bar{f}(s) ,$$

$$\bar{\Delta T}_s = \bar{T}_{s_{x=0}} - \bar{s}^{-1} T_0 = \bar{s}^{-1} a + b \bar{f}(s) .$$

But eq.20, which is an appropriate general solution for T_s in a semi-infinite solid, shows that

$$\bar{f}(s) = k_s \sqrt{s/k_s} B(s) ,$$

$$\bar{s}^{-1} a + b \bar{f}(s) = B(s) ,$$

whence it follows that

$$B(s) = \bar{s}^{-1} a \{ 1 - b k_s \sqrt{s/k_s} \}^{-1} .$$

This is precisely the form of $B(s)$ given in eq.22, where we identify the constants a and b as follows :

$$a = \Delta T / (1+Q)$$

$$-b = (\rho \Gamma)_{av} Q \sqrt{k_s} / (1+Q) \sqrt{\beta} k_s = \sqrt{\tau} / \sqrt{\rho_s C_s k_s} .$$

The function $f(t)$ is just q_s as given in eq.26 and is the only function of t which satisfies eqs.28.



precisely the same dependence upon the dimensionless time t/τ and differ only in their amplitudes. It will be shown below that the V_o output given in eq.34 can be accurately extrapolated back to the point where $t/\tau = 0$, thus giving a direct measure of the quantity $c\{\alpha V\Delta T/R(1+Q)\}(\tau\delta)^{-1/2}$. Eq.32 shows that the thermometer gauge output V_g is given by

$$V_g = \frac{\alpha V\Delta T}{(1+Q)} \{1 - e^{t/\tau} \operatorname{Erfc} \sqrt{t/\tau}\} \quad 35$$

and the amplitude of this function can be easily determined too. It follows that a knowledge of c and δ leads to a direct evaluation of the characteristic time τ . Measurement of the primary shock speed permits evaluation of ΔT so that, with a knowledge of α and κ it is possible to obtain a simultaneous measurement of Q and hence of the thermal conductivity of the gas.

The experimental determination of the amplitudes in eqs.34 and 35 proceeds as follows. Writing

$$c.A. \frac{1}{\sqrt{\tau\delta}} = B ; \quad A = \frac{\alpha V\Delta T}{(1+Q)} ; \quad f(t/\tau) = e^{t/\tau} \operatorname{Erfc} \sqrt{t/\tau} \quad 36$$

$$\text{we have} \quad V_g = A(1 - f(t/\tau)) \quad , \quad 37$$

$$V_o \sim B f(t/\tau) \quad . \quad 38$$

Fig.4 is a sketch of a typical experimental record, showing the analogue and thermometer-gauge outputs to the same time scale. For times greater than some time t_o , which depends on the character of the apparatus and which will be discussed more fully in a later section, the experimental outputs are assumed to be given by eqs.37 and 38. Taking any pair of times $t_1, t_2 > t_o$, the intervals ΔV_o and ΔV_g are determined. It follows from eqs.37 and 38 that

$$\frac{|\Delta V_g|}{|\Delta V_o|} = \frac{A}{B} = \frac{\sqrt{\tau\delta}}{c} = \chi \quad 39$$

The ratio χ is a constant, independent of the values of t_1 and t_2 (provided that they are $> t_o$.) It can be seen that experimental confirmation of the constancy of χ provides confirmation that the foregoing theory is accurate.

Once χ is found it is a simple matter to add χ times the V_o -output ordinates to the V_g -output ordinates, and thus to locate the asymptote A . The value of the intercept of the V_o -trace with the V_o axis, namely B , follows directly.

$$V_o = \frac{V_g}{1 + \chi} + B$$

The experimental values of the ordinates of the V_g trace are added to χ times the ordinates of the V_o trace to locate the asymptote A . The value of the intercept of the V_o -trace with the V_o axis, namely B , follows directly.

$$V_o = \frac{V_g}{1 + \chi} + B$$

$$(1 + \chi)V_o = V_g + \chi B$$

$$V_o + \chi V_o = V_g + \chi B$$

The experimental values of the ordinates of the V_g trace are added to χ times the ordinates of the V_o trace to locate the asymptote A . The value of the intercept of the V_o -trace with the V_o axis, namely B , follows directly.

$$\chi = \frac{V_g - V_o}{V_o - B}$$

The value of χ is a constant, independent of the value of V_g . It can be seen that experimental measurements of the ordinates of the V_g trace and the V_o trace are sufficient to determine χ and B .

3. Experimental Details

The shock tube used for these tests is made from stainless steel of 5.08 cm internal diameter and one cm wall thickness, mounted vertically with the high pressure section at ground level and the working section at first floor level. The dump chamber and vacuum equipment are on the second floor. Since reflected shock waves were being studied the shock tube was terminated with a plug holding the resistance thermometer 5.12 m from the diaphragm section. The high pressure section was 1.22 m long. A small two stage mechanical vacuum pump was used to reduce the pressure in the tube and is capable of an ultimate pressure of about 10^{-2} Torr. The normal sequence of operation was to reduce the pressure in the tube to about this value and then admit atmospheric air via a small silica gel drier until the desired pressure was reached. The pressure was read on a Texas Instrument fused quartz pressure galvanometer with a 0 - 100 cm Bourdon tube. This instrument is most useful for shock tube work since the required pressure can be set on a digital counter and gas admitted until a null reading is obtained. The leak rate into the tube was about 1×10^{-2} Torr/min which was negligible when compared with the lowest pressure of 100 Torr and times, from vacuum shut-off to diaphragm burst, of about 2 minutes. High pressure bottled nitrogen was used as the driver gas with maximum driving pressures up to 25 atm.

The primary shock Mach numbers covered the range 1.5 to 3.5. The lower Mach numbers at low initial tube pressures were produced with weak diaphragms, made from 0.12 mm thick Melinex*. It was found possible to scribe this material with a wheel type glass cutter so that it would burst at low pressure differentials down to about 2 atm. Half hard aluminium sheet 0.45 mm thick was used for the higher Mach numbers and a range of bursting pressures from 4 atm up to 25 atm was obtained by scribing the sheet to various depths. For this the glass cutter was preloaded with different weights.

The shock velocity was measured one metre upstream of the reflecting end of the tube by detecting its passage over two thin film resistance thermometers set flush with the walls of the tube and spaced 20 cm apart. The output of the detectors is amplified via transistorised

* Melinex - Imperial Chemical Industries Terylene sheet

pulse amplifiers and these signals start and stop a digital chronometer. The time intervals are measured to ± 0.1 μ sec. The Mach number was obtained from the velocity by using the speed of sound in dry air appropriate to the ambient conditions.

Gauges

Surface temperatures on the end face were measured with thin film resistance thermometers. These were made by painting platinum paint (Hanovia 05X*) onto a glass substrate in the form of microscope slides which were readily available. They appeared to be a medium hard glass with a softening temperature about 700°C. The films were formed by drawing the desired shape of the thermometer with a draughting pen. After a short interval of air drying the glass was placed in a cold electric furnace. The temperature was raised to 500°C with the door left open to ensure adequate ventilation as a mildly oxidising atmosphere is necessary in the early stages of film formation. The door was then closed, the temperature was raised to 650°C, and the glass was allowed to soak for 5 min at this temperature, after which it was removed and allowed to cool in the open air. Current leads were formed by painting lines of silver paint (flake silver type FSP4**) connecting the ends of the platinum to two soldering points on the opposite side of the glass and following a firing sequence similar to above with a maximum temperature of 600°C.

Copper wires were soldered to the silver leads and the gauge was mounted in the end plug of the shock tube using vacuum wax and ensuring that the gauge surface presented to the shock wave was normal to the geometrical axis of the tube.

The moderate gas temperatures envisaged in these tests indicated that the surface temperature rise to be measured would only be a few degrees. A simple analysis shows that thin film resistance thermometers are best operated at high resistance and low current, rather than low resistance and high current, since this enables the gauges to be run at a much lower power dissipation resulting in a lower equilibrium surface temperature and long life. (Thin film gauges used for shock detection in this shock tube are run under these conditions and are still in use after over 2000 firings of the tube.)

* Englehard Industries, Vauxhall Street, London

** Johnson Matthey Ltd., Hatton Garden, London

Gauges were produced in an overall area of 1.2 cm square with lengths of 16 - 17 cm and resistances of about 1000 Ω by having a zig zag arrangement. Ten milliamps through these gauges resulted in equilibrium temperatures about 10°C above ambient.

Detection Equipment

A fast rise time for the associated electronic equipment was necessary to preserve the rapid response capability of the thin film thermometers and to give adequate resolution in the oscilloscope display times of 10 microseconds. Some type of cathode follower was obviously indicated with gauges of high resistance and the best performance was obtained with a field effect transistor (Fairchild MOS FI 100) connected as a source follower. This transistor has an input capacitance of less than 1 pF and was mounted within one cm of the gauge. The transistor was run from a battery power supply of 18 volts. The gate of the FI 100 is isolated from the substrate by a thin layer of metal oxide which gives the transistor its low input capacitance and high input impedance (of the order of 10^{15} ohms). This oxide layer is easily ruptured if excessive voltages (greater than about 40 volts) are applied to the gate and hence the battery power supply for the gauge was limited to 36 volts, because in a simple constant current supply the full supply voltage will appear across the gauge if it open circuits (a not unlikely event in the shock tube). With a supply voltage which is not very much greater than the gauge voltage the current is no longer constant and it follows that the resistance change R_g is related to the voltage output V_g of the gauge by

$$\frac{R_g}{R} = \frac{V_g}{V} \left(1 + \frac{R}{R_s}\right) \quad 40$$

R is the original gauge resistance, V the standing voltage across the gauge and R_s is the series resistance to give the required current.

The output from the source follower was connected to a Tektronix 1121 pre-amplifier (maximum gain 100, bandwidth 5 c/s to 17 Mc/s) and thence directly to one beam of a Tektronix 551 double beam oscilloscope, via a type L plug in unit.

Analogue

The technique described above for determining the asymptotic temperature rise required an analogue network with rapid response time. The constant lump size T - section network shown in figure 3 was built with high stability $3.3 \text{ k}\Omega \pm 1\%$ resistors and $47 \text{ pF} \pm 1\%$ mica capacitors. The circuit values were determined by the requirement that the first resistor, $1.65 \text{ k}\Omega$, should be large compared with the output resistance of the pre-amplifier (93Ω) and small compared with the input resistance of the type L amplifier in the oscilloscope ($1 \text{ M}\Omega$), The capacitive elements of the network were limited to the preferred value of 47 pF as this gave a sufficiently short analogue time constant of 38 n sec and it was felt that the capacity would be large enough so that stray capacities would have little effect. The network had 48 equal sections giving an output equivalent to an infinite section network for a running time of $70 \mu \text{ sec}$.

The output of the analogue is obtained by measuring the voltage developed across the first resistor of the network. It is usual to do this with differential amplifiers but these are limited in response time. For these tests the analogue was connected directly across the L amplifier with point A (figure 3) earthed. The input capacity of the L amplifier is 20 pF which is large when compared with the 47 pF of the network and hence a second source follower was used to reduce this capacity to a minimum (less than 1 pF). The output of the analogue, via the source follower, was displayed on the second beam of the Tektronix 551 oscilloscope.

The complete electronic circuit is given in figure 5. The equipment was calibrated for overall risetime and gain by injecting a signal from a Tektronix 107 square wave generator (rise time 3 n sec) in series with the actual gauge mounted in the shock tube. The rise time was found to be about $26 \mu \text{ sec}$ and the gain of the source followers about 0.9. The gain in the rest of the system was determined by the calibrated dial settings.

Gauge Calibration

The surface temperature is obtained from the oscilloscope trace via the relation

$$\Delta T = \frac{R}{\alpha R} \frac{E}{R}$$

α is the temperature coefficient of resistance defined as

$$\alpha = \frac{1}{R_1} \frac{R_1 - R_0}{T_1 - T_0}$$

The suffix 0 refers to a reference condition and was taken as that relevant to the equilibrium conditions of the gauge in the shock tube.

α was determined by passing a highly stabilised current of 1 mA through the gauge and measuring the voltage across the gauge with a digital voltmeter (resolution 10 μ V). The gauge was immersed in a small volume of silicone oil and heated in a water bath to cover a temperature range of about 20°C. It is not possible to calibrate these high resistance gauges in air since they behave as the equivalent of sensitive hot wires. Silicone oil is very suitable as it has no observable short or long term effect on the resistance of the gauge. The temperature coefficients determined in this way ranged between 1.56 °C⁻¹ and 1.66 °C⁻¹ for the microscope slide substrate. It is interesting to note that α is very dependent on the type of glass used and is significantly higher for Pyrex at 2.3 °C⁻¹.

The specific heat C_s , the thermal conductivity k_s and the density ρ_s of the substrate must be known in order to calculate Q.

There is a large weight of evidence which shows that the thermal properties of the substrate, when determined dynamically in time intervals comparable with shock tube running times, are significantly different from handbook values. Skinner (1962) gives 3.63×10^{-2} cal cm⁻² °C⁻¹ sec^{1/2} accurate to $\pm 5\%$ for $\sqrt{\rho c k_s}$ for both Pyrex and quartz whereas the handbook value for Pyrex is 3.03×10^{-2} and that for quartz is 3.58×10^{-2} . It is obviously necessary to make a direct measurement of $\sqrt{\rho_s c_s k_s}$ and the very elegant variation of the joule heating method as used by Skinner was adopted. Briefly, a pulse of current is passed through the gauge which then changes its resistance as the heat which it has produced diffuses into the substrate. This is done with the gauge in air and then with the gauge immersed in a liquid. Skinner shows that the thermal properties of the substrate are given by

$$\sqrt{\rho_s c_s k_s} = \sqrt{\rho_l c_l k_l} \left(\frac{A^1}{A} - 1 \right)^{-1}$$

where the suffix l refers to the liquid

A^1 is the amplitude of the oscilloscope trace with the gauge in air and A is the amplitude of the trace with the gauge in liquid, both amplitudes being determined at the same time. This technique is independent of the waveform of the heating current and the only requirement is that the currents are identical in the two cases.

Water is a natural choice for the calibrating liquid as its properties are well known. Furthermore, $\sqrt{\rho c k}$ for water is 3.80×10^{-2} , a value very close to the value for glass, this, giving maximum accuracy. Unfortunately, unless the gauges are sealed from water by a thin coating of silicon monoxide (required primarily to insulate the gauge from ionised gas flows) they suffer a permanent change of resistance after being immersed in water. Silicon monoxide was not used in these tests since it was undesirable; for example a practical layer of thickness only 1000\AA increases the response time by about one μsec . It was not possible to use water, therefore, and a different inactive liquid had to be found. Glycerol, with a value of 2.22×10^{-2} , and silicone oil type *MS 200/100 cs with a value of 1.12×10^{-2} seemed suitable and were readily available. Both liquids have been used successfully giving a mean value for the microscope slide substrate of 3.61×10^{-2} and having no apparent adverse effect on the gauge.

The circuit used to produce the constant current pulse is shown in figure 6. To obtain measurable outputs only portions of the gauges (about 100Ω) could be calibrated at a time. The actual output is superposed on a very large signal and the bridge must be carefully balanced. If the waveform amplitudes are to be compared, the initial zero positions must be identical. Skinner overcame the inaccuracies arising from any initial unbalance, by using an extended current pulse, and taking the amplitudes towards the end of the oscilloscope trace. This was not deemed advisable in this case, because it was felt that the calibration period should be comparable with the shock tube observation time. Consequently a display time of 200 microseconds was used. In this time interval, and with approximately equal arms in the bridge network, the heat transfer to the substrate is constant. One dimensional heat flow analysis shows that the surface temperature, i.e. gauge resistance, should vary as \sqrt{t} under these conditions. The experimental results show that this is so to a high degree of accuracy and this fact has been used to

* Midland Silicones,
Reading.

determine the original zero position of the trace. The bridge was balanced by trial and error, allowing sufficient time between pulses for the gauge and substrate to return to an equilibrium condition. When an acceptable balance had been achieved the oscilloscope trace was recorded. The gauge was then immersed in the calibrating liquid and a slight readjustment of the balance was required. This change of zero position is thought to be due to the liquid always being slightly below ambient temperature, and was equivalent to a change in resistance of about 0.1% (temperature difference about 0.5°C). After approximate rebalancing the second trace was recorded on the same film. The time origin could be accurately defined and the amplitudes from the two traces relative to a nominal zero were plotted on a \sqrt{t} scale. Two straight lines resulted, the slopes of which gave the required amplitude ratios.

4. Discussion

Typical oscilloscope traces for two different conditions of primary shock Mach number and initial tube pressure are shown in figure 7. Details of the technique for obtaining the asymptotic temperature rise and the characteristic accommodation time are given at the end of section 1. A tracing of the experimental record given in the previous illustration has been reproduced to an enlarged scale in figure 8, together with the appropriate values of A, B, and τ . Within the experimental accuracy the constancy of the asymptotic value confirms that the theoretical model gives an accurate description of the experiment for times $t \geq \tau$. It should be noted that the experimental curve departs markedly from theory at the beginning of the trace, giving the appearance of a prolonged rise time. This is typical of all traces and may be due to any, or all, of mechanical, electrical, or gas dynamical influences.

From measurements of the primary shock speed, initial tube pressure and temperature, the pressure and temperature T_{∞} in the reflected shock region were calculated using ideal gas relations ($\gamma = 1.4$). The voltage A (see figure 8, for example) was used to calculate the asymptotic value of ΔT_s and this quantity, together with the value of ΔT , was sufficient for evaluation of the experimental $\sqrt{\rho c k}$ ratio, Q (see equations 23 to 25). Figure 9 shows the experimental variation of Q with p. It is known that Q is proportional to $1/\sqrt{p}$ and the experimental results are consistent

with this fact. The best fit for a line with slope $-\frac{1}{2}$ gives a value for Q of 300 at a pressure of one atmosphere. The experimental points cover a mean temperature (defined as $\frac{1}{2}(T_{\infty} + T_0)$) range from 380°K to 500°K . In the theoretical work, Q has been assumed to be independent of temperature, and in the present set of experiments no attempt has been made to take account of the small temperature variations which are, in fact, known to be present.

The thermal conductivity of the gas was evaluated as follows. Using the thermal equation of state it is easily seen that,

$$\rho k C_p = \frac{C_p}{k} \cdot p \cdot \frac{k}{T}.$$

Therefore, putting $\gamma = 1.4$, we have (see e.q. 24)

$$\frac{k}{T} = \rho_s k_s C_s / 3.5 Q^2 p,$$

and with a value for $\sqrt{\rho_s k_s C_s}$ equal to $3.60 \times 10^{-2} \text{ cal cm}^{-2} \text{ }^{\circ}\text{K}^{-1} \text{ sec}^{-\frac{1}{2}}$ it transpires that

$$\frac{k}{T} = 1.53 \times 10^{-2} \cdot Q^{-2} \cdot p^{-1}. \quad (p \text{ in atmospheres})$$

This quantity was evaluated for each experimental point in figure 9. The conductivity, k , was then calculated at the mean temperature for that particular experiment, and plotted in figure 10. The points scatter about the accepted values taken from the Smithsonian tables (Forsythe, 1954), the great majority being within $\pm 10\%$. A more accurate evaluation of k would be possible if greater attention was paid to obtaining values for Q at specific mean temperatures. However, this is a difficult procedure with normal shock tube operation, but will be attempted when a greater mass of experimental data is available. Figure 10 also illustrates the accuracy of the assumption made about the thermal conductivity in the theory. On the whole, the results in figure 10 are satisfactory and with a little more refinement, as indicated, the technique should yield reasonable estimates of the thermal conductivity.

The accommodation coefficients evaluated from this series of experiments are exhibited in figure 11, and can be seen to be generally around and below a value of 0.1. It is this low value which causes the effects of accommodation to occur within a readily observable time interval (see equations 5 and 27). A least-squares fit to the experimental points shows that the accommodation coefficient varies as $1/\sqrt{p}$, to a close approximation. For this reason it is tempting to speculate that this links the accommodation coefficient with the fraction of sites which are available for adsorption when the molecular species are adsorbed as dissociated atoms.

It must be emphasised that the measured accommodation coefficients apply to a thin film (approximately 0.5μ thick) of platinum deposited from china paint on to a glass substrate. The state of the surface is not known, and although it has the appearance of bright polished platinum, the authors would be hesitant to state categorically that the results could be applied to pure platinum. Nevertheless, it is interesting to note the apparent correlation between the present data and that available for nitrogen at pressures lower by four orders of magnitude (see figure 12).

In conclusion, the present series of experiments provides good evidence that thermal accommodation processes are responsible for the experimental observations. With the knowledge gained so far, there seems every prospect for exploitation of the technique for measurement of surface effects at very much higher pressures and temperatures than those which have been possible with existing methods.

The authors are grateful for the enthusiastic cooperation of R.A. Briggs during the course of these experiments.

REFERENCES

- Baganoff, D. (1965) J. Fluid Mech., 23, 2, 209-228.
- Clarke, J.F. (1960) College of Aeronautics Rept. 124.
- Clarke, J.F. (1962) J. Fluid Mech., 13, 1, 47-64.
- Clarke, J.F., McChesney, M. (1964) "The Dynamics of Real Gases",
Butterworths, London.
- Erdélyi, A. et al (1954) "Tables of Integral Transforms", Vol. 1.
New York, McGraw Hill Book Co. Inc.
- Forsythe, W.E. (1954) Smithsonian Physical Tables. 9th ed.
Smithsonian Institution, Washington.
- Friedman, H.S., Fay, J.A. (1965) Physics of Fluids, 8, 11, 1968-1975.
- Goldsworthy, F.A. (1959) J. Fluid Mech., 5, 2, 164.
- Hansen, C.F., Early, R.A., Alsfon, F.E., Witterborn, F.C.,
(1959) NASA TR R-27.
- Hansen, C.F. (1960) ARS Jour., 30, 10, 942-946.
- Lauver, M.R. (1964) NASA TN D-2117.
- Meyer, R.F. (1960) National Research Council of Canada,
Aero. Rept., LR - 279.
- Meyer, R.F. (1963) National Research Council of Canada,
Aero. Rept., LR - 375.
- Peng, T.-C., Ahtye, W.R. (1961) NASA TN D-687.
- Skinner, G.T. (1962) Cornell Aeronautical Laboratory
Rept. No. CAL - 105.
- Wachman, H.Y. (1962) J. Am. Rocket Society., 32, 1, 2 - 12.

APPENDIX. Evaluation of V_o .

The voltage output of the analogue is given as a Laplace transform in eq.33 above. We can write

$$V_o = \frac{\alpha V \Delta T}{R(1+Q)} \cdot \frac{1}{\sqrt{\tau}} \cdot I \quad A1$$

where

$$I = \frac{1}{2\pi i} \int_L \frac{e^{ts} ds}{\sqrt{s(s+\delta)} [\sqrt{s} + \sqrt{1/\tau}]} \quad A2$$

and L is the usual Laplace transform inversion contour. Deforming L into a loop contour around the negative real-part-of- s -axis it can be shown that

$$I = \frac{1}{\pi\sqrt{\tau}} \int_0^{\delta} \frac{e^{-tu} du}{\sqrt{u(\delta-u)} (u+1/\tau)} - \frac{1}{\pi} \int_{\delta}^{\infty} \frac{e^{-tu} du}{\sqrt{u-\delta} (u+1/\tau)} \quad A3$$

$$= \frac{1}{\sqrt{\tau}} e^{-\frac{1}{2}\delta t} \int_0^{\infty} e^{-(\frac{1}{2}\delta + \frac{1}{\tau})u} I_0\left[\frac{1}{2}\delta(t+u)\right] du - \frac{e^{t/\tau} \operatorname{Erfc}\sqrt{(\delta+1/\tau)t}}{\sqrt{\delta + 1/\tau}} \quad A4$$

I_0 is the zero-th order modified Bessel function and eq.A4 is in an especially suitable form for evaluation under the condition $\delta t \gg 1$. The last term in eq.A4 is $O(\exp(-\delta t))$ and, using the asymptotic series for I_0 in the first integral, it is found that

$$\begin{aligned} \sqrt{\delta} I &\sim \left\{ 1 - \frac{1}{2}(\delta\tau)^{-1} + \frac{3}{8}(\delta\tau)^{-2} - \dots \right\} e^{t/\tau} \operatorname{Erfc} \sqrt{t/\tau} \\ &+ \frac{1}{2} \frac{(\delta\tau)^{-1}}{\sqrt{\pi t/\tau}} \left\{ 1 - \frac{3}{4}(\delta\tau)^{-1} + \dots \right\} \\ &+ \frac{3}{16} \frac{(\delta\tau)^{-2}}{\sqrt{\pi(t/\tau)^3}} + \dots \end{aligned} \quad A5$$

Eq.A5 shows that the error in the analogue output is negligible ($< 1\%$) in the regions (roughly $t \geq \tau$) where it applies. (N.B. $\delta\tau$ is typically of order 10^{-1} .)



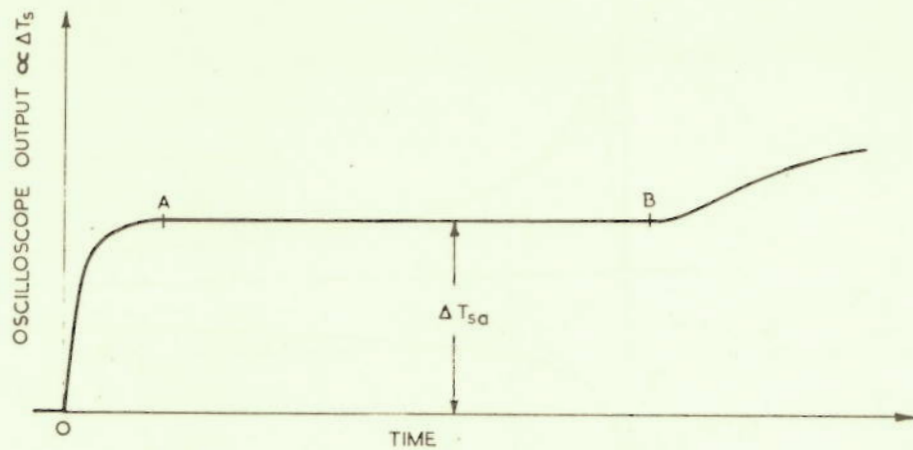


FIG 1. OSCILLOSCOPE TRACE FROM A THIN FILM RESISTANCE THERMOMETER MOUNTED ON THE END WALL OF A SHOCK TUBE. (SCHEMATIC)

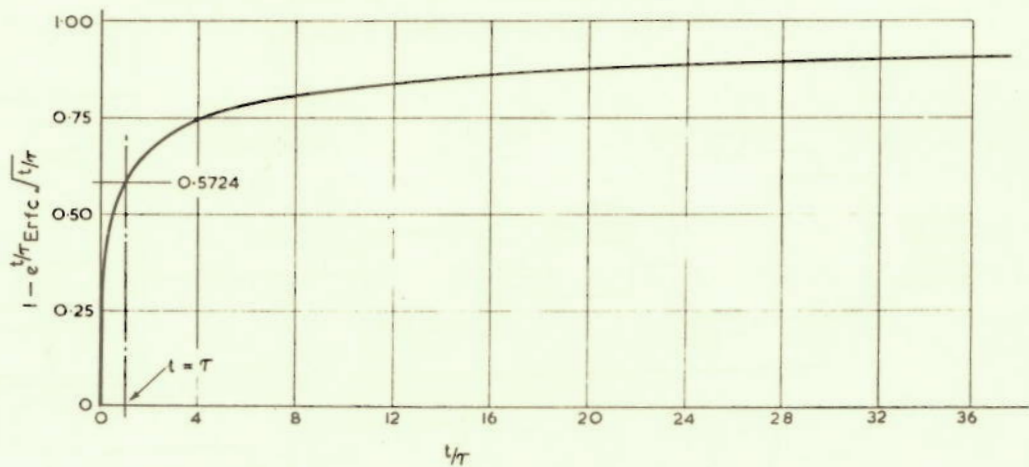


FIG 2. THE FUNCTION $e^{-t/\tau} \text{Erfc} \sqrt{t/\tau}$. τ IS THE CHARACTERISTIC TIME FOR SURFACE ACCOMMODATION.

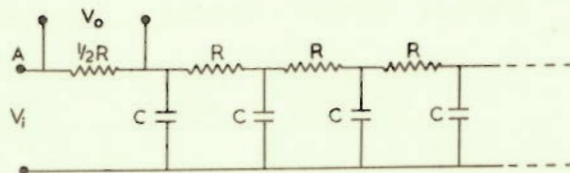


FIG 3. ANALOGUE NETWORK.

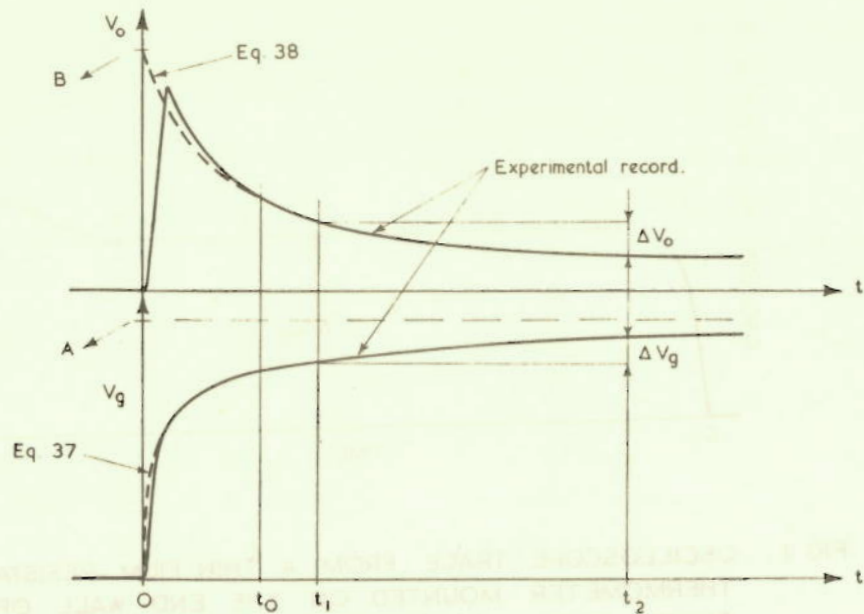


FIG 4. DETERMINATION OF A AND B FROM THE EXPERIMENTAL RECORD.

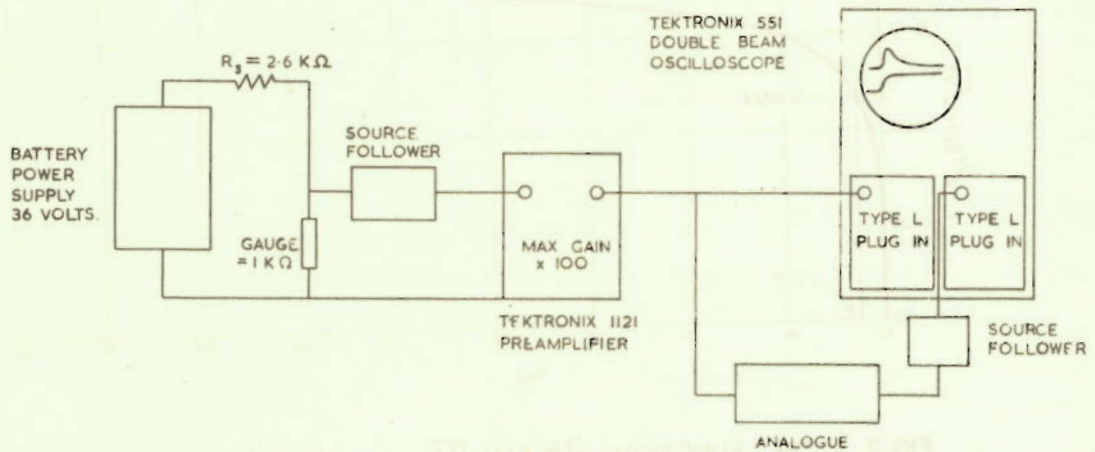


FIG 5. DIAGRAMMATIC LAYOUT OF GAUGE AMPLIFIER AND DISPLAY CIRCUIT. OVERALL RISETIME = 26 n secs.

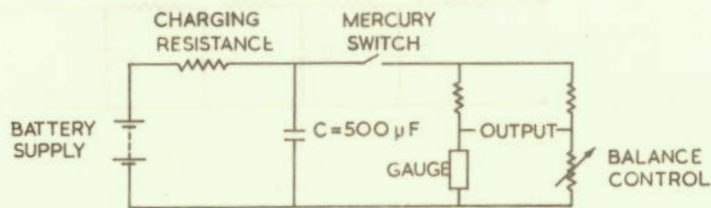


FIG 6. SUBSTRATE CALIBRATION CIRCUIT.

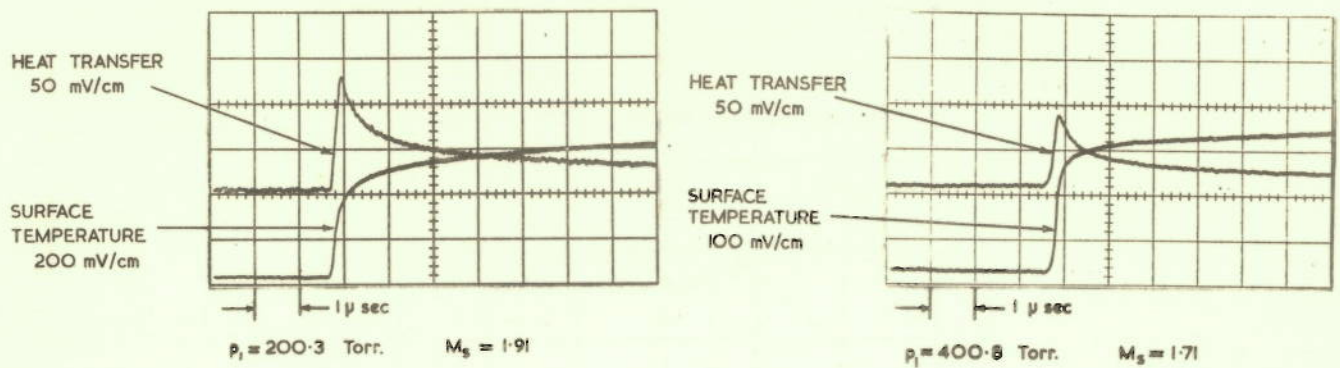


FIG 7. TYPICAL OSCILLOSCOPE RECORDS.

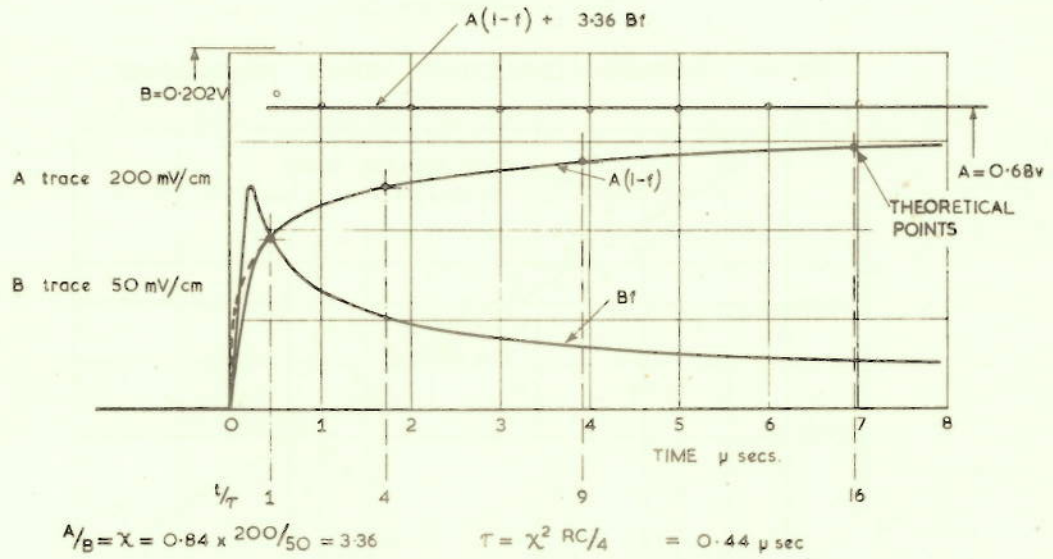


FIG 8. REDUCTION OF TYPICAL OSCILLOSCOPE TRACE.
 $p_1 = 200.3$ Torr. $M_s = 1.91$

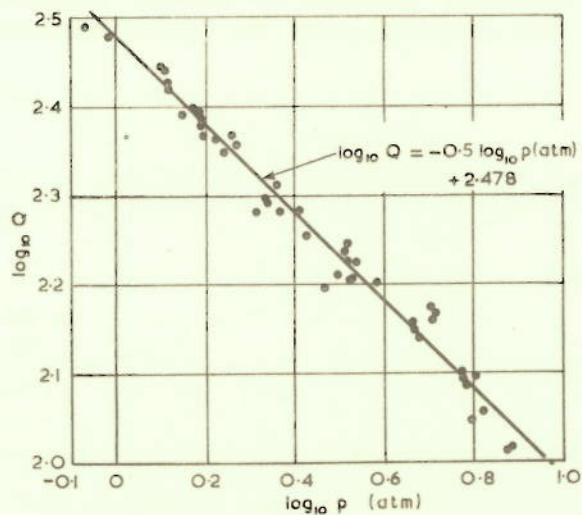


FIG 9. EXPERIMENTAL VALUES OF THE $\sqrt{p}ck$ RATIO.

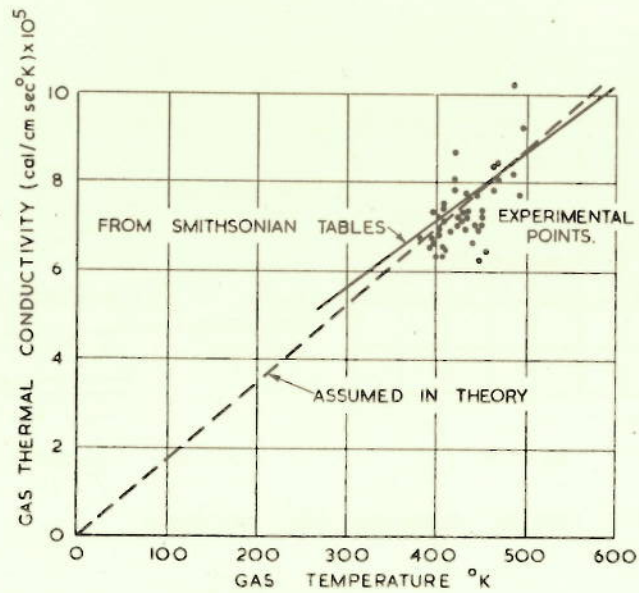


FIG 10. THERMAL CONDUCTIVITY VERSUS TEMPERATURE.

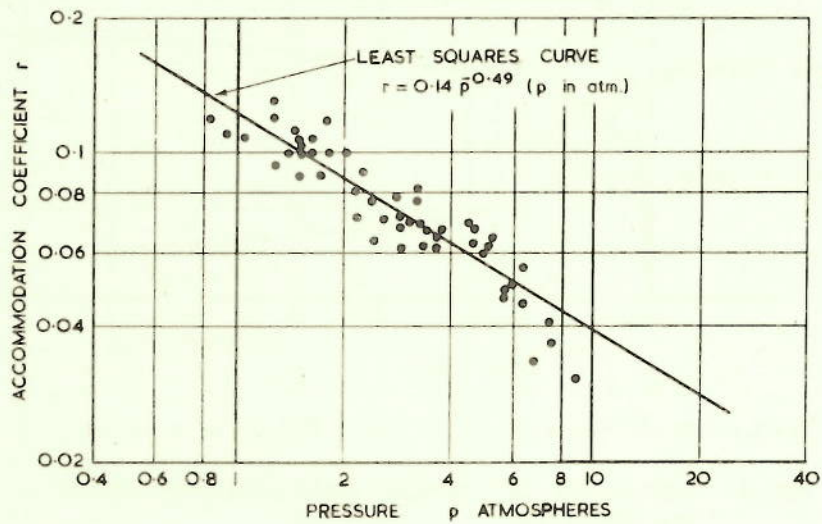


FIG 11. MEASURED VARIATION OF SURFACE ACCOMMODATION WITH PRESSURE — AIR ON BRIGHT PLATINUM.

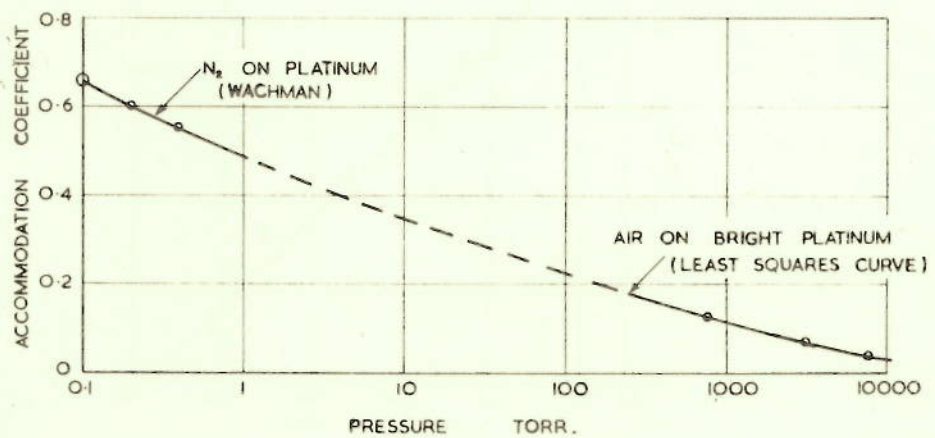


FIG 12. COMPARISON OF PRESENT DATA WITH RESULTS GIVEN BY WACHMAN.